

# Automated inspection and classification of flip-chip contacts using Scanning Acoustic Microscopy

S. Brand<sup>a</sup>, P. Czurratis<sup>b</sup>, P. Hoffrogge<sup>b</sup>, M. Petzold<sup>a</sup>

<sup>a</sup> Fraunhofer Institute for Mechanics of Materials, Halle, Germany

<sup>b</sup> PVA TePla Analytical Systems GmbH, Aalen, Germany

---

## Abstract

*Industrial applications often require failure analysis methods working non-destructively, enabling either a rapid quality control or fault isolation and defect localization prior to detailed defect investigation requiring target preparation. Scanning acoustic microscopy in the frequency range above 100 MHz provides high axial and lateral resolution, a moderate penetration depth and the required non-destructivity. In this study a method for an automated detection of defects in flip-chip contacts was developed. Chip samples were manufactured in flip-chip technology containing a 750  $\mu\text{m}$  thick die with solder balls (80  $\mu\text{m}$  diameter) on top of the substrate. For acoustic inspection a scanning acoustic microscope in combination with a 175 MHz transducer was used. Recorded echo signals were analyzed off-line applying custom-made MATLAB software. For differentiation between flip-chip contacts and the underfill, the recorded echo signals were pre-analyzed. Signals obtained from the contacts were then inspected by wavelet-, pulse separation- and backscatter amplitude integral analysis. Complementary X-ray- and SEM inspection was performed for defect verification. The separation of pulses obtained at the interfaces of the contacts, the absolute values and the distribution of wavelet coefficients corresponded to the interconnecting condition. The success rate of detecting voids was 96.8% as verified by SEM imaging, while manual X-ray inspection showed success only in 64% of the analysed cases.*

---

## 1. Introduction

Flip-Chip technology combined with solder bump interconnections is applied widely in electronic device manufacturing. For ensuring the connective reliability, appropriate failure analysis methods for non-destructively inspecting the electrical contacts are needed. Due to power dissipation thermally induced mechanical stress is a major issue for the reliability of bonded and soldered interfaces [2], [4], [5]. Several techniques for inspecting interconnections in electronic circuits including optical systems, X-ray microscopy, scanning electron microscopy, strength testing and microsection analysis are available. Scanning acoustic microscopy however, is of increasing interest due to its unique ability to illuminate optically opaque materials, providing depth-specific information and to locally evaluate mechanical properties. Moreover, acoustic microscopy is working non-destructively, which allows the application of several test procedures at a single device [1]. The goal of the current work was the development of an automated working application for a non-destructive estimation of quality related parameters of flip-chip interconnections in electronic devices. Time resolved scanning acoustic microscopy in the frequency

range between 150 – 175 MHz was applied. From recorded unprocessed ultrasound rf-signals appropriate signal parameters were derived and related to the contacts condition. Connective defects were detected automatically using specific parameter ranges of the backscatter amplitude integral (BAI) [3], pulse separation characteristics and the distribution of the wavelet coefficients, estimated from the rf-signals.

## 2. Material and Methods

### 2.1. Scanning Acoustic Microscopy

Scanning acoustic microscopy is a powerful tool for non-destructively deriving depth-specific information of optically non-transparent samples combined with a lateral resolution in the  $\mu\text{m}$ -range. Employed was an acoustic microscope (Evolution II, PVA TePla Analytical Systems GmbH, Aalen, Germany) equipped with a 175 MHz transducer. Scanning was performed with an increment of 4  $\mu\text{m}$  in the lateral x- and y-directions, while the transducer tip and the sample were immersed in distilled water at room temperature for wave coupling. Echoes were

digitized at a sampling rate of 500 MS/s and stored on the microscopes internal hard drive. Data files containing unprocessed rf-signals were then transferred to a desktop computer and off-line analysis was performed.

Samples inspected were CPU-devices manufactured in flip-chip technology containing solder bumps (80  $\mu\text{m}$  – lateral diameter) for connecting the silicon chip to the die-attach of the CPU. The silicon had a thickness of approx. 750  $\mu\text{m}$  with a surface area of 20 mm x 30 mm.

## 2.2 Signal Analysis

Signal analysis of the rf-echoes was performed using a custom-made MATLAB (The Mathworks, Natick, USA) software. The lateral locations of the bumps were estimated by differentiating between the interfaces silicon-connector and silicon-underfill using characteristic reflective features of these interfaces as illustrated in fig.1. Figure 1-right shows the Hilbert transformed cross section of the sample. Echoes occurring at the silicon-connector interface were considerably longer than echoes from the silicon-underfill interface. Parameter values of the backscatter amplitude integral (BAI) were computed within the time range between the exit echo of the silicon and the signal peak at the bump-connector/die-attach interface as indicated by the red rectangle in fig. 1. Further analysis was applied to signals of the bump-interconnections exclusively. These included Wavelet analysis with a Gaussian mother wavelet of the 4<sup>th</sup> order for deriving wavelet coefficients versus scaling factors and time. Moreover, relative peak positions and the corresponding pulse widths of the silicon-bump interface were evaluated. Finally, all parameters were combined in a classification model for deriving a binary void-intact decision of flip-chip connectors. To provide a simplified visual indication the resulting decision matrix was color coded and superimposed to the BAI-parametric image

## 2.3 Complementary Defect Verification

During the method development locations of defect bump contacts were estimated using X-ray microscopy (XD7600, Dage). From the known void positions ultrasonic data were acquired and signal parameters were computed for comparison to parameter values obtained at known intact connectors. Characteristic parameter ranges were derived from the acoustic data and implemented in the analysis algorithm. Following, the success rate of the acoustic defect estimation was evaluated using “unknown” samples. Void positions were estimated from the ultrasonic data and the binary decision matrix was computed. Both, X-ray and scanning electron microscopy (TM1000, Hitachi) was applied in order to verify the results.

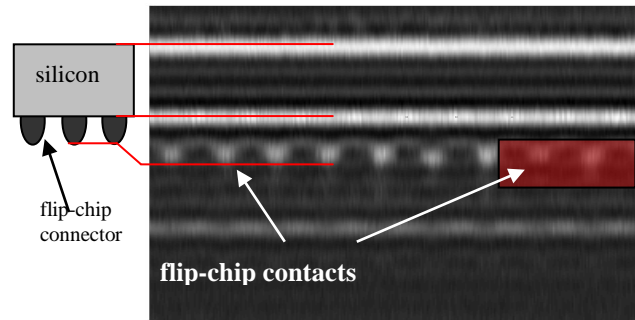


Figure 1: Sample description. The scheme on the left illustrates the 750  $\mu\text{m}$  silicon layer with the flip-chip contacts underneath. On the right a cross-section image through the CPU-device is shown. Boundaries and corresponding echoes are indicated by red lines. The red rectangle shows the time range for estimating BAI values.

## 3. Results and Discussion

Connector localization: According to the cross-section image in Fig. 1 interconnect positions were located using the pulse length of the echo obtained at the silicon-connector interface. In presence of a contact the peak amplitude of the echo at the silicon-connector interface was 200% higher compared to the signals at the interface silicon-underfill. The pulse width obtained from a connector was 30 ns while the echo at the silicon-underfill interface was only 10 ns long. Defect classification: Wavelet analysis was applied to the echo signals recorded at the silicon-interconnect interface. Significant differences in the distributions of the wavelet coefficients were observed between intact and defect flip-chip connectors. Wavelet coefficients estimated from a void showed broader distributions versus scaling factors and wavelet positions compared to values obtained from an intact contact. In case of a void wavelet coefficients of equal amplitude occur almost homogeneously over all wavelet positions. The average distribution width over the scaling factors (sf) was 1.7sf for intact connectors and 2.5sf for the voids. Distributions were estimated at 70% of the maximum values. The second parameter included in the classification was the relative position of the signal peak at the silicon-connector interface. Pulse shifts of up to 20 ns between intact and defect contacts were observed. Both parameters were combined in a classifier for increasing the success rate and to optimize for false-positive classifications. Figure 2 shows the results estimated by the classifier. Green indicated spots in Fig. 2-left specify positions of intact bump-connectors. Voids and false positive contact positions are marked red. The settings and parameter ranges applied for computing the results in Fig. 2-left were optimized for classification of the

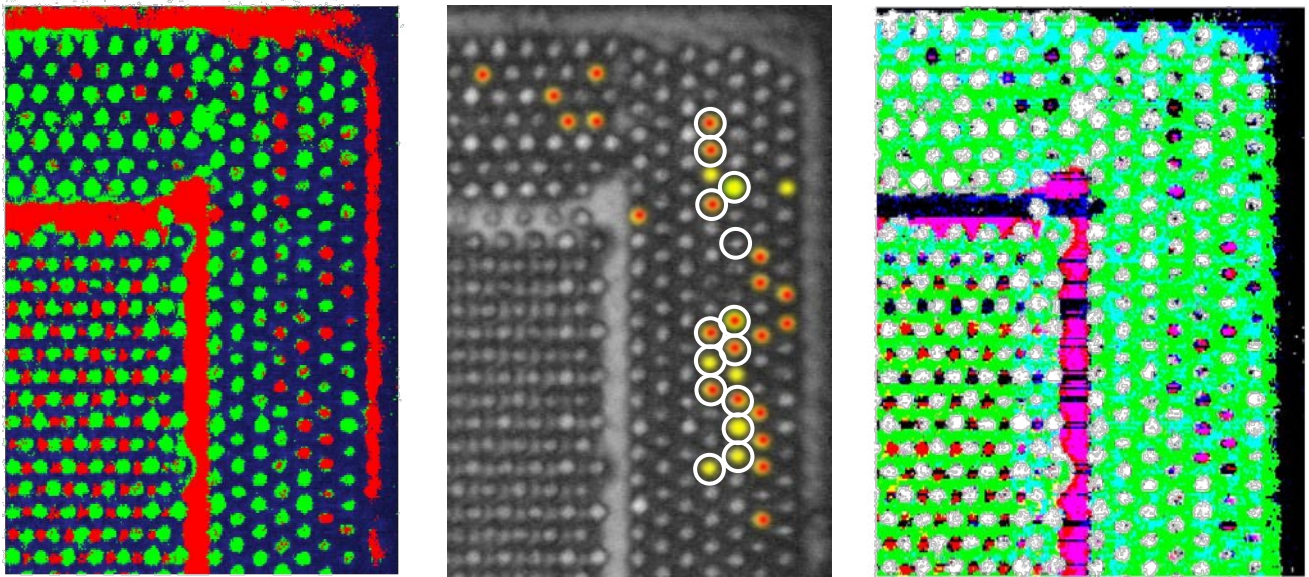


Figure 2: Classification results and evaluation of void detection. Left: green indicated are extracted flip-chip connectors. Red connectors were classified as voids based on the wavelet coefficients and pulse separation characteristics at the interface silicon/connector. Middle: BAI-parametric image with indication of detected voids. Yellow marks correspond to voids detected using acoustic microscopy data. Red marks indicate where voids were confirmed by X-ray microscopy. White circles indicate where defect connections were verified by cross-sectioning and SEM imaging. SEM investigations were only performed on column 3 and 4 (counted from the right-hand-side of the device). Right: superimposed parameter maps. Red indication corresponds to pulse separation in the “void-range”. Blue marks indicate the wavelet coefficients and green stains everything that is not detected as a connector.

flip chip-connectors at the outer rim of the device. The application of adapted settings is required in order to classify the inner interconnects.

For evaluating the reliability of the acoustic based inspection and classification method complementary X-ray- and scanning electron microscopy (SEM) was performed. The decision map (figure 2-left, 2-middle) was given to a technical assistant experienced in void detection using the X-ray. In Figure 2-center all acoustically detected voids are indicated yellow. Red indication in Fig. 2-center corresponds to voids confirmed by X-ray. It can be seen that 8 out of 31 voids estimated from the acoustic data were not confirmed. In addition to X-ray SEM was applied to the rows of connectors with the highest number of voids detected. Voids revealed by SEM are indicated by a white circle in Fig. 2-middle. It can be seen that thirteen voids detected by the ultrasonic method were verified by SEM. However, it also shows that two false-positive and one false-negative detections occurred, which corresponds to an overall success rate of 90.3%.

The acoustically based method developed here showed good performance in classifying flip-chip contacts in an automated way. It seemed superior to complementary X-ray inspection by a trained person. Further experiments

will be performed in the near future for optimizing the methods reliability.

#### Acknowledgements

The authors also thank Natalie Yeo for technical assistance with the defect evaluation by X-ray microscopy and the SEM imaging.

#### References

- [1] A. Briggs, *Advances in Acoustic Microscopy*. New York and London, Plenum Press, 1995.
- [2] S.C. Omathuna, T. Fromont, W. Koschnick and L. Oconnor, “Test Chips, Test Systems, and Thermal Test Data for Multichip Modules.” in the Esprit-Apachip Project, 1994.
- [3] K. Raum, A. Ozguler, S.A. Morris and W.D. O'Brien, “Channel defect detection in food packages using integrated backscatter ultrasound imaging.” *IEEE Transactions on Ultrasonics Ferroelectrics and Frequency Control*, vol. 45(1), pp. 30-40, 1998.
- [4] H. Reichl, “Packaging aspects of single and multichip modules.” In *Proceedings of the 1st European Conference on Electronic packaging Technology (EuPac 1994)*, German Welding Society, pp. 6-9, 1994.
- [5] G.L. White, “An introduction to die attach.”, *Welding Institute research Bulletin*, pp. 268-271, 1981